



## Assessment of the impacts of cloud chemistry on surface SO<sub>2</sub> and sulfate levels in typical regions of China

Jian-yan Lu<sup>1</sup>, Sunling Gong<sup>1,5\*</sup>, Chun-hong Zhou<sup>1\*</sup>, Jian Zhang<sup>1</sup>, Jian-min Chen<sup>2,3,4</sup>, Lei Zhang<sup>1</sup>

5

<sup>1</sup> State Key Laboratory of Severe Weather, Key Laboratory of Atmospheric Chemistry of CMA, Institute of Atmospheric Composition, Chinese Academy of Meteorological Sciences, Beijing 100081, China

<sup>2</sup> Shanghai Key Laboratory of Atmospheric Particle Pollution and Prevention (LAP3), Department of Environmental Science and Engineering, Fudan Tyndall Centre, Institute of Atmospheric Sciences, Fudan University, Shanghai, China

10 <sup>3</sup> Center for Excellence in Urban Atmospheric Environment, Institute of Urban Environment, Chinese Academy of Science, Xiamen, China

<sup>4</sup> Shanghai Institute of Eco-Chongming (SIEC), No.3663 Northern Zhongshan Road, Shanghai 200062, China

<sup>5</sup> National Observation and Research Station of Coastal Ecological Environments in Macao, Macao Environmental Research Institute, Macau University of Science and Technology, Macao SAR 999078, China

15

\* Corresponding authors.

*E-mail addresses:* [Sunling.Gong@cma.gov.cn](mailto:Sunling.Gong@cma.gov.cn) (S Gong), [zhouch@cma.gov.cn](mailto:zhouch@cma.gov.cn) (C Zhou)

### Abstract

A regional online chemical weather model WRF/ CUACE (China Meteorological Administration Unified Atmospheric  
20 Chemistry Environment) was used to assess the contributions of cloud chemistry to the SO<sub>2</sub> and sulfate levels in typical regions in China. By comparing with several time series of in-situ cloud chemical observations on Mountain Tai in Shandong Province of China, the CUACE cloud chemistry scheme was found to well reproduce the cloud processing the consumptions of H<sub>2</sub>O<sub>2</sub>, O<sub>3</sub> and SO<sub>2</sub>, and consequently was used in the regional assessment for a heavy pollution episode and monthly average in December 2016. During cloud availability in heavy pollution episode, the sulfate production increases 40-80% and SO<sub>2</sub>  
25 reduces over 80%. During the heavy pollution episode, it is found that the cloud chemistry mainly affects the middle and lower troposphere below 5 km as well as within the boundary layer, and contributes significantly to SO<sub>2</sub> reduction and sulfate increase in east-central China. Among the regions of North China Plain (NCP), Yangtze River Delta (YRD) and Sichuan Basin (SCB), the SCB is mostly affected by the cloud chemistry, with the average SO<sub>2</sub> abatement up to about 1-15 ppb and sulfate increase up to more than 50 μg m<sup>-3</sup>, followed by YRD where the contribution of cloud chemistry is still significant, averaging  
30 up to 1-3 ppb for SO<sub>2</sub> abatement and 5-20 μg/m<sup>3</sup> for sulfate increase. The cloud chemistry contribution to PRD and NCP are not significant and weaker than other two regions due to lighter pollution and less water vapor, respectively. In addition, the average contribution of cloud chemistry during the pollution period was significantly greater than that for all December. This



study provides a way to analyze the over-estimate phenomenon of SO<sub>2</sub> in many chemical transport models.

35 Keywords: SO<sub>2</sub>, sulfate, cloud chemistry, WRF/CUACE

## 1 Introduction

Aerosols interact with radiation and clouds, directly or indirectly affecting the atmospheric radiation balance and precipitation, which in turn affects weather and climate (Twomey et al., 1984; Twomey, 1991; Charlson et al., 1992; Ramanathan et al., 2001; Pye et al., 2020). Moreover, large amounts of aerosols dispersed in the atmosphere can reduce  
40 visibility and deteriorate air quality (Molina, 2002), which is harmful to human health (Xie et al., 2019; Sielski et al., 2021).

In addition to direct emissions, aerosols are mostly produced secondarily through the oxidation of precursor gases, and one of the important processes is the transformation in clouds. Global cloud coverage of about 21% to 95% provides an adequate environment for cloud chemistry processes (Kotarba, 2020; Ravishankara, 1997). As about 90% of the clouds formed in the atmosphere evaporate without deposition or forming the precipitation, large fractions of aerosols formed in them can  
45 then also enter the atmosphere (Caffrey et al., 2001; Harris et al., 2013; Lelieveld et al., 1992). Globally, sulfate production from SO<sub>2</sub> oxidation accounts for about 80% of total sulfate, and more than half of this sulfate is produced in clouds (Hung et al., 2018; Faloon et al., 2010; Guo et al., 2012). Ge et al. (2021) calculated the contribution of cloud chemistry to global SO<sub>2</sub> contribution, and found that cloud chemistry processes reduced SO<sub>2</sub> concentrations by 0 ~ 50% in most of east-central China in all seasons. In China, Li (2011) found that the average SO<sub>4</sub><sup>2-</sup> concentration in cloud water accounted for 53.8% of the total  
50 aerosol concentration at a Mount site. Li et al. (2020) also found that cloud processes effectively reduced atmospheric O<sub>3</sub> and SO<sub>2</sub> concentrations by an average of 19.7% and 71.2%, respectively, at Mount Tai.

In addition to the observations, model simulations are an important way for cloud chemistry at different spatial-temporal scales. GEOS-Chem, CMAQ, WRF-Chem, CCAMx, ESM2, and other models have all been used to study the cloud chemical processes on SO<sub>2</sub> and sulfate (Tremblay and Leighton, 1986; Ge et al., 2021; Ervens, 2015; Shimadera et al., 2011) and the  
55 complex homogeneous, inhomogeneous and multiphase reactions in clouds due to the complex mixture of gaseous, liquid and solid phases (Pye et al., 2020; Ravishankara, 1997; Liu et al., 2021).

There has been very serious air pollution in central-east China where four heavy pollution regions of North China Plain (NCP), Yangtze River Delta (YRD), Sichuan Basin (SCB) and Pearl River Delta (PRD) are located (Yao et al., 2021; Zhang et al., 2012). Although many global and regional models include sulfate formation mechanisms in cloud chemistry, few models  
60 have assessed its contribution, especially the lack of detailed assessment of regional cloud chemistry on sulfate and SO<sub>2</sub> in



China and those pollution regions. Many regional chemical transport models have reported the results of SO<sub>2</sub> over-estimate problems (Buchard et al., 2014; He et al., 2015; Wei et al., 2019; Sha et al., 2019; Georgiou et al., 2018). The inadequate inclusion or lack of cloud chemistry of SO<sub>2</sub> consumption simulations is one of the main problems (Ge et al., 2021). Therefore, there is a very important need to accurately quantify the contribution of cloud chemistry in these regions and the central-east  
65 China when it comes to heavily polluted weather to get a better understand of multi-dimensional pollution distributions, especially in the upper layer besides the surface.

This study is intended to use an on-line coupled chemical weather platform of CMA: WRF/CUACE, to analyze and evaluate the SO<sub>2</sub> in-cloud oxidation process in the four regions, with two objectives: (1) evaluating the cloud chemistry scheme in WRF/CUACE by the in-situ cloud chemistry observations at Mount Tai in summers of 2015 and 2018; and (2) quantifying  
70 the contributions of cloud chemistry to the SO<sub>2</sub> and sulfate changes in a typical winter pollution month of December 2016. It is aimed to establish a system to assess the relative contribution of cloud chemistry to SO<sub>2</sub> oxidation pathways and sulfate productions to other clear-sky processes.

## 2 Model description and Methodology

### 2.1 Cloud chemistry in WRF/CUACE

75 WRF/CUACE is an on-line coupled chemical transport model under the WRF frame work with a comprehensive chemical module – CUACE, which was developed at CMA with a sectional aerosol physics, gas chemistry, aerosol-cloud interactions and thermodynamic equilibrium (Zhou et al., 2012; Zhou et al., 2016; Gong et al., 2003; Gong and Zhang, 2008; Zhang et al., 2021). There are seven types of aerosols, i.e. black carbon, organic carbon, sulfate, nitrate, ammonium, soil dust, and sea salt, and more than 60 gaseous species. The aerosol size spectrum was divided into 12 bins with fixed boundaries of  
80 0.005-0.01, 0.01-0.02, 0.02-0.04, 0.04-0.08, 0.08-0.16, 0.16-0.32, 0.32-0.64, 0.64-1.28, 1.28-2.56, 2.56-5.12, 5.12- 10.24 and 10.24-20.48 μm. The system can simulate PM<sub>10</sub>, PM<sub>2.5</sub>, O<sub>3</sub> and visibility. The cloud chemistry mechanism in CUACE is a scheme developed by Salzen et al. (Gong et al., 2003; Von Salzen et al., 2000), which considers the oxidation of SO<sub>2</sub> by H<sub>2</sub>O<sub>2</sub> and O<sub>3</sub> in both stratocumulus and convective clouds. The transport and chemical effects of sulfur in convective clouds are calculated based on a convective cloud model by WRF. Within the cloudy part of a grid box, the first-order rate constant (in s<sup>-1</sup>)  
85 of S(IV) oxidation is given by the following expression:

$$F = \left| \frac{1}{C_{S(IV)}} \frac{dC_{S(IV)}}{dt} \right| = F_1 C_{O_3} + F_2 C_{H_2O_2} \quad (1)$$

where C<sub>S(IV)</sub> is the total concentration of S(IV) (gas phase plus dissolved), C<sub>O<sub>3</sub></sub> is the total concentration of O<sub>3</sub>, and C<sub>H<sub>2</sub>O<sub>2</sub></sub> is the



total concentration of hydrogen peroxide.

The effective rate constants  $F_1$  and  $F_2$  are given by the following expressions:

$$90 \quad F_1 = R_{O_3} f_1 \quad (2)$$

$$F_2 = R_{H_2O_2} f_2 \quad (3)$$

The reaction rate constants  $R_{O_3}$  and  $R_{H_2O_2}$  refer to Maahs (1983) and Martin et al. (1984):

$$R_{O_3} = \{4.4 \times 10^{11} \exp(-4131/T) + 2.6 \times 10^3 \exp(-966/T) [H^+]^{-1}\} (Ms)^{-1} \quad (4)$$

$$R_{H_2O_2} = 8 \times 10^4 \exp[-3650(1/T - 1/298)] \{0.1 + [H^+]\}^{-1} (Ms)^{-1} \quad (5)$$

95 In Equations (2) and (3), the factors  $f_1$  and  $f_2$  represent the partitioning of the substance between the aqueous and gas phases and are determined by the Henry's law coefficients.

$$f_1 = \gamma f_{SO_2} f_{O_3} K_S \bar{K}_{HO} \quad (6)$$

$$f_2 = \gamma f_{SO_2} f_{H_2O_2} \bar{K}_{HS} \bar{K}_{HP} \quad (7)$$

where  $\gamma$  is the dimensionless volume fraction of liquid water in the cloud. The parameters  $f_{SO_2}$ ,  $f_{O_3}$  and  $f_{H_2O_2}$  are the  
100 proportions of individual substances in the gas phase. They are calculated from the dimensionless Henry's law constant and  $\gamma$ .

$$f_{SO_2} = (1 + \gamma \bar{K}_{HS} K_S)^{-1} \quad (8)$$

$$f_{O_3} = (1 + \gamma \bar{K}_{HO})^{-1} \quad (9)$$

$$f_{H_2O_2} = (1 + \gamma \bar{K}_{HP})^{-1} \quad (10)$$

with

$$105 \quad K_S = \bar{K}_{HS} \left( 1 + \frac{K_{1S}}{[H^+]} + \frac{K_{1S}K_{2S}}{[H^+]^2} \right) \quad (11)$$

The Henry's law constants used in (6) to (8) are listed in table 1.

In order to consider the dependence of the oxidation rates on the pH, the  $H^+$  concentration is calculated from ions balance.

$$[H^+] + [NH_4^+] = [OH^-] + 2[SO_4^{2-}] + 2[SO_3^{2-}] + [HSO_3^-] + [NO_3^-] + [HCO_3^-] [H^+] + [NH_4^+] = [OH^-] + 2[SO_4^{2-}] + 2[SO_3^{2-}] + [HSO_3^-] + [NO_3^-] + [HCO_3^-] \quad (12)$$

110 Eqs. (1) ~ (12) can be used to calculate the oxidation rates of  $SO_2$  by the oxidants  $H_2O_2$  and  $O_3$  in the liquid environment in the cloud in CUACE and the transformations of sulfate. In CUACE, the equilibrium constant  $K_{HS}$  has been corrected from 1.23 to  $1.23 \times 10^{-3}$  and added it into the cloud chemistry. At the same time, all the unit in those cloud chemical formula in Table 1 have been checked and unified in terms of the original references to make them reasonable.

## 2.2 Assessment criteria

115 To assess the effect of the cloud chemistry mechanism on  $SO_2$  and sulfate, three variables, RTCLD, DT, and RT, are



defined. The RTCLD is defined as the ratio of chemical species before and after the cloud chemistry mechanism.

$$RTCLD(i) = 1 - \frac{BECLD(i)}{AFCLD(i)} \quad (13)$$

where  $i$  denotes the chemical component of  $\text{SO}_2$ ,  $\text{O}_3$ ,  $\text{H}_2\text{O}_2$ , and sulfate, hereafter. The BECLD denotes the concentration of component  $i$  before cloud chemistry, and the AFCLD after the cloud chemistry.

120 The DT indicates the difference in concentration of substance  $i$  with (CLD) and without (CCLD) cloud chemistry.

$$DT(i) = CLD(i) - CCLD(i) \quad (14)$$

The RT represents the concentration ratio change of the substance  $i$  with and without cloud chemistry:

$$RT(i) = 1 - \frac{CCLD(i)}{CLD(i)} \quad (15)$$

## 2.3 Methodology

### 125 2.3.1 Model Evaluation – Case 1

Mount Tai with an altitude of about 1500 m, located in central Shandong Province, is the high point of the North China Plain. As the Riguan Peak of Mount Tai is far from pollution sources, and the water vapor conditions in summer favors very much cloud formations, it is an ideal observation site for cloud chemistry observation (Li et al., 2017; Li et al., 2020a; Li et al., 2020b). The observed concentrations of  $\text{SO}_2$ ,  $\text{O}_3$  and  $\text{H}_2\text{O}_2$  in cloudy conditions from June 19 to July 30, 2015 and from June 130 20 to July 30, 2018 with time interval of 1 h were obtained to evaluate the cloud chemistry scheme in WRF/CUACE (Li et al., 2017; Li et al., 2020a; Li et al., 2020b).

WRF/CUACE is set with two-domain nested for the evaluation, with the Riguan Peak as the central point (Fig. 1a). The horizontal resolution of outer domain (O) is 9 km with  $100 \times 104$ , and of the inner domain (I) is 3 km with  $88 \times 94$  (Fig. 1a).

There are 32 vertical layers with the top pressure of 100 hPa.

### 135 2.3.2 Simulations of Regional Characteristics – Case 2

In order to assess the regional contribution of cloud chemistry to  $\text{SO}_2$  and sulfate in CUACE, December 2016 was selected with a widespread heavy pollution episode occurred in North and East China from Dec. 16 to 21 and covering NCP, YRD and SCB with the highest hourly fine particulate matter ( $\text{PM}_{2.5}$ ) concentration exceeding  $1100 \mu\text{g m}^{-3}$  (Yuan and Ma, 2017). The simulation region is set up as shown in Figure 1b also with two-level domain nesting. The outer domain (O) covers 140 Central and East Asia with a horizontal resolution of 54 km and a grid of  $139 \times 112$ . The inner domain (I) covers most of China on the eastern side of the Qinghai-Tibet Plateau with a horizontal resolution of 18 km and a grid of  $157 \times 166$ . The vertical layer number of the model is the same as that in the Case 1.



Since the cloud water is the reaction pool of cloud chemistry, whether the simulation of cloud water is reasonable or not is directly related to the effectiveness of cloud chemistry. Both the cloud water and rainwater from WRF are coupled to the cloud chemistry module and main physics configurations are listed in Table 2.

#### 2.4 Meteorological and Satellite Data

For both cases, the meteorological initial boundary values for WRF/CUACE were from NCEP (National Centers for Environmental Prediction) FNL global reanalysis at a resolution of  $1^\circ$  with 6-h interval. The chemical lateral boundary conditions were from NOAA (National Oceanic and Atmospheric Administration) Meteorological Laboratory Regional Oxidant Model (NALROM) (Liu et al., 1996). The model was run in a restart way with a 5-day spin-up.

FY-2G cloud image data of CMA with an 1 h interval was used to evaluate the cloud in both cases. Routine observations in 3 h interval from 31 meteorological stations of CMA and hourly pollution observations from 31 stations of the China General Environmental Monitoring Station were used to evaluate the meteorological fields and pollutants for December 2016. Meteorological elements include 2 m air temperature, 2 m relative humidity, and 10 m wind speed.

This study uses the MEIC inventory as the default anthropogenic emissions, with  $0.25^\circ$  spatial resolution, including the emissions of sulfur dioxide ( $\text{SO}_2$ ), nitrogen oxides ( $\text{NO}_x$ ), carbon monoxide (CO), ammonia ( $\text{NH}_3$ ), black carbon (BC), organic carbon (OC), non-methane volatile organic compounds (NMVOCs),  $\text{PM}_{2.5}$  and  $\text{PM}_{10}$  by five sectors of power, industry, transportation, residential, and agriculture (Li et al,2017; Zheng et al,2018). The emission sets for years of 2015 and 2017 were used for Case-1, of 2016 for Case-2, respectively.

### 3 Results and Discussions

#### 3.1 Evaluation of the cloud chemistry mechanism

In order to verify the cloud chemistry mechanism in WRF/CUACE, the simulations were compared with the cloud chemistry observations at Mount Tai. By analyzing the distribution of satellite cloud images in and around Mount Tai and matching with the observed data, two time periods with clouds from June 19 to July 30, 2015 and June 20 to July 30, 2018 were selected for the comparative analysis, defined as "cloud process-1" (CP-1) and "cloud process-2" (CP-2), respectively. The statistics of correlation coefficients (R), relative average deviation (RAD), and normalized mean deviation (NMB) between hourly simulated and observed  $\text{SO}_2$ ,  $\text{O}_3$ , and  $\text{H}_2\text{O}_2$  are shown in Table 3. The results show that the RADs of  $\text{SO}_2$ ,  $\text{O}_3$  and  $\text{H}_2\text{O}_2$  in CP-1 and CP-2 are in the range of 2% ~ 30%, and the simulated and observed averages are within the same magnitude and close to each other. Among them, the simulated and observed averages of  $\text{SO}_2$  were very close in both CP-1 and



170 CP-2, with RAD below 10 %. The R for the three species are 0.77, 0.49 and 0.72 for CP-1, and 0.49, 0.46 and 0.03 for CP-2, respectively. The analysis reveals that although the correlation of H<sub>2</sub>O<sub>2</sub> in CP-2 is only 0.03, the RAD is -2 % and the NMB is 5.1 %. All the above results show that SO<sub>2</sub> and two important oxidants O<sub>3</sub> and H<sub>2</sub>O<sub>2</sub> are reasonably simulated in both time periods.

It is also found that when cloud chemistry occurs, SO<sub>2</sub> concentration values range from 0-3 ppbv, mostly less than 1 ppbv, O<sub>3</sub> in the range of 25-125 ppbv, and H<sub>2</sub>O<sub>2</sub> in the range of 0-100 μM (Fig. 2) in clouds. All three species are agreed within a factor two of observed concentrations. In addition, CP-2 shows increased concentrations of both oxidants of O<sub>3</sub> and H<sub>2</sub>O<sub>2</sub>, compared to CP-1. The SO<sub>2</sub> concentrations are small for both time periods. Shen et al. (2012) found mean SO<sub>2</sub> concentrations of 8.1 ppbv and 6.4 ppbv for the Mount Tai site in summer 2007 and 2008. Li et al. (2020) observed that the yearly mean summer SO<sub>2</sub> concentrations of 1.3 ± 1.1 ppbv, 0.3 ± 0.2 ppbv, and 0.4 ± 0.2 ppbv in 2014, 2015, and 2018, respectively. The average O<sub>3</sub> concentrations were 50.3 ± 10.9 ppbv, 73.1 ± 19.7 ppbv and 66.3 ± 18.3 ppbv, respectively. The mean H<sub>2</sub>O<sub>2</sub> concentrations were 11.6 ± 13.1 μM, 22.8 ± 13.1 μM, and 45.1 ± 29.5 μM, respectively. Besides, H<sub>2</sub>O<sub>2</sub> concentrations were 0.55 ± 0.67 ppbv in 2007 (Ren et al., 2009), 0.93 ± 1.01 ppbv in 2018 (Ye et al., 2021), 2.05 ± 1.20 ppbv in 2019 (Ye et al., 2021). The results of our simulations are consistent with the trends of other observational studies, which indicates an increase in the atmospheric oxidation and a decrease in the SO<sub>2</sub> concentration.

185 Figure 3 shows the satellite cloud maps, simulated column cloud and simulated liquid water content at 8:00 LST on June 24, and 8:00 LST on June 25 in CP-1. The results indicate that not only the simulated column cloud but also the cloud liquid water distribution simulated at the two times are consistent with the satellite observations.

Figure 4 shows the RTCLD of SO<sub>2</sub> and simulated liquid water contents at 2:00 and 8:00 LST on June 24, and 2:00 and 8:00 LST on June 25 in CP-1. The results indicate that the RTCLD of SO<sub>2</sub> distribution simulated at the four times are consistent with the cloud liquid water, so for the distribution of RTCLD of SO<sub>2</sub> with a reduction of more than 80% within the cloud region of Mount Tai and most of Shandong province, which is consistent with the cloud chemistry observation studies by Li (2020).

In summary, the cloud chemistry mechanism in WRF/CUACE is reasonable to reproduce the cloud chemistry for the gaseous pollutant SO<sub>2</sub> and the important oxidants of O<sub>3</sub> and H<sub>2</sub>O<sub>2</sub>. The model not only simulates the concentrations of the three species, but also the SO<sub>2</sub> decreasing trend and O<sub>3</sub> and H<sub>2</sub>O<sub>2</sub> increasing trends with year.

### 3.2 Assessment of the cloud chemistry impacts on regional SO<sub>2</sub> and sulfate

This session will further assess the contribution of cloud chemistry for the four main pollution regions of NCP, YRD,



PRD, and SCB (Fig. 1) in China for the whole December of 2016 and a pollution episode occurred during this period (Dec. 16-21) as Case 2.

### 200 3.2.1 Meteorological evaluation

As the driving force of air pollution and cloud chemistry, the meteorological conditions simulated in the four major pollution regions (Table 4) were evaluated with observations. The correlations of all elements with observations were very close in both the whole December and the heavy pollution in four regions, indicating that the model performed well both in December and the heavy pollution episode. The temperature correlation is the best in December, followed by humidity and then wind speed which is consistent with previous researches (Zhou et al., 2012; Wang et al., 2015; Gao et al., 2016). The RMSEs of wind speeds all range from 1.03 to 1.50 m s<sup>-1</sup>, falling within the criteria (less than 2 m s<sup>-1</sup>) to define “good” model performance in stagnant weather proposed by Emery et al. (Emery et al., 2001). The RSME of wind speed during heavy pollution is smaller than that of December, which indicates that the model can well performance the static wind even though it is very small.

210 Figure 5 shows the satellite cloud image, simulated column cloud and simulated liquid water content for the maturation and dissipation stages of the episode. The satellite image shows that the cloud coverage region is mainly in the southwest including SCB on the 19<sup>th</sup>, almost covers most of eastern China including NCP, YRD, PRD and SCB on the 20<sup>th</sup> and the 21<sup>st</sup>, and then move eastward outside of China on the 22<sup>nd</sup> (Fig.4 a1-d1). The simulated clouds fit well with the satellite images (Fig.4 a2-d2). Since the cloud chemistry occurs in the cloud area, the cloud chemistry mainly affects three regions of NCP, 215 YRD and SCB of the four pollution regions as PRD has relatively much less cloud. The column liquid water distribution also moves from west to east as the episode develops (Fig.5 a3-d3), but is located more southern part of eastern China than that of the cloud. In SCB and YRD, there is more abundant in liquid water content, which can reach more than 500 g m<sup>-2</sup>, while in PRD There is slightly less, up to 100 g m<sup>-2</sup>, and in NCP there is the least liquid water content, 0.1 g m<sup>-2</sup> mostly due to the dry environment and partly due to the overestimated temperature and underestimated humidity in Table 4.

220 The above analysis shows that the model basically reproduces the meteorological field in December and heavy pollution periods, which provides a better meteorological background basis for the effective simulation of pollution as well as cloud chemistry.

### 3.2.2 Pollutants Evaluation

The simulated hourly PM<sub>2.5</sub>, O<sub>3</sub>, and SO<sub>2</sub> concentrations in four regions were also compared with the observations (Table 225 5). The simulations are all within a factor of two of the observations (figure omitted), and the mean values of the three





pollutants simulated in the four regions are very close to the observations, indicating that model captures well the variability of  $PM_{2.5}$ ,  $O_3$  and  $SO_2$  concentrations during both December 2016 and the heavy pollution episode.  $O_3$  correlates well with observations in all four regions.  $PM_{2.5}$  is better simulated in three regions, NCP, YRD and PRD, and worse in SCB.  $SO_2$  performs better in YRD and PRD, and relatively worse in NCP and SCB. All the three pollutants are better simulated in YRD and PRD during the heavy pollution episode than those for December averages. The following section of this paper will focus on assessing the impact of cloud chemical processes.

### 3.2.3 Assessment of regional contributions

The regional impacts of cloud chemical processes on surface  $SO_2$  and sulfate were analyzed for whole December and for a pollution episode of Dec. 16-21. The pollution episode was investigated with respect to the maturity stage (21:00 LST on Dec. 20 - 17:00 LST on Dec. 21) and to the dissipation stage (2:00 LST on Dec. 22) for the four pollution regions NCP, YRD, PRD, and SCB.

The average effect of cloud chemistry on surface  $SO_2$  and sulfate in December (Fig. 6,  $DT(SO_2)$  and  $DT(\text{sulfate})$ ) was simulated. It is found that  $SO_2$  declination in December is concentrated mostly in the central-eastern part of China, by an average of 0.1-0.5 ppb in most regions there. The SCB was maintained as a relatively stronger center by declining 1.0-5.0 ppb, far more than other areas. NCP has no obvious declination center, while YRD has a smaller scatter declination center. Correspondingly, sulfate growth is mainly centering in SCB and other areas along the Yangtze River, with the maximum center up to 10-30  $\mu\text{g}/\text{m}^3$  in most part of SCB and 3-10  $\mu\text{g}/\text{m}^3$  in the Yangtze River. In contrast, there are no obvious growth centers in NCP and PRD.

The spatial distribution of cloud chemistry contribution to  $SO_2$  and sulfate during the whole mature stage of the heavy pollution was analyzed (Fig. 7,  $DT(SO_2)$  and  $DT(\text{sulfate})$ ) on the 19<sup>th</sup> to the 21<sup>st</sup>. It shows that  $SO_2$  decreased the most in the SCB, exceeding 1-3 ppb in most area, to 3-15 ppb in the central region, and also up to 1-3 ppb in most area of the YRD, while the NCP and PRD decreased the least, below 1 ppb in most area. The regional distribution of sulfate increase and  $SO_2$  consumption is roughly anticorrelated, but still with difference. Sulfate increases by more than 10  $\mu\text{g}/\text{m}^3$  in the area of from southern of the NCP to central China and from most of the eastern part of the SCB to YRD. Sulfate increases more than 20  $\mu\text{g}/\text{m}^3$  in the SCB with up to more than 50  $\mu\text{g}/\text{m}^3$  in the center, while 5-20  $\mu\text{g}/\text{m}^3$  in YRD and 3-5  $\mu\text{g}/\text{m}^3$  in PRD without obvious growth center. In NCP, the southern part about 5-20  $\mu\text{g}/\text{m}^3$ , but most part less than 3  $\mu\text{g}/\text{m}^3$ .

Comparing the contribution of cloud chemistry in the whole December with the pollution maturity stage of 19-21, it shows that cloud chemistry in heavy pollution weather for  $SO_2$  depletion and sulfate increase is mainly concentrated in the



central-eastern part of China, and the four major pollution regions are also more obvious. However, SO<sub>2</sub> consumption and  
255 sulfate increase are not consistent, which is not only influenced by the local SO<sub>2</sub> concentration, but also by the cloud amount.  
Therefore, for SCB, which is less polluted and has much more clouds than NCP, the effect of cloud chemistry on sulfate and its  
precursor SO<sub>2</sub> is always the most significant in the SCB, both during heavy pollution and averaged over the whole December.

Exploring details into the pollution episode, it is found that the cloud chemistry influence was mainly on SCB and YRD at  
21:00 LST on Dec. 20. The sulfate concentration increases (RT(sulfate)) by about 10-40 µg/m<sup>3</sup> in most parts of SCB, and the  
260 highest is about 150-225 µg/m<sup>3</sup> in its southwest (Fig. 8a). The increase is about 10-40 µg/m<sup>3</sup> in most parts of YRD, with 5-10  
µg/m<sup>3</sup> in some parts of its northwest, and the highest increase can reach 100-150 µg/m<sup>3</sup>. At 21<sup>st</sup> 17:00 LST, it shows that the  
pollution episode has moved eastward and the cloud chemistry process has a stronger impact on NCP, YRD, PRD than that of  
the previous time (Fig. 8b). The increase center is located in Shandong Province, with up to 100-150 µg/m<sup>3</sup>, and with about 1-5  
µg/m<sup>3</sup> in most of NCP. In PRD, it has been influenced the least by the cloud process with sulfate concentration increase of 5-40  
265 µg/m<sup>3</sup> scattering partly only in some regions. At 22<sup>nd</sup> 12 LST, although the episode has gradually dissipated, it still had an  
impact on SCB and YRD with sulfate increase about 10-40 µg/m<sup>3</sup> in most of these areas (Fig. 8c).

Above all, the contribution of cloud chemistry to surface sulfate during this pollution process is the highest in the SCB,  
followed by the NCP and YRD, with maximum concentration increases of 225 µg m<sup>-3</sup>, 150 µg m<sup>-3</sup>, and 40 µg m<sup>-3</sup>, respectively,  
and sulfate increases of 10-40 µg m<sup>-3</sup> in most regions of these three areas.

270 Further analysis of the simulation characteristics of cloud chemistry on all the regions during the pollution maturity stage,  
i.e., the cloud process from Dec. 19 to 21, was investigated (Table 6). It can be seen that cloud chemistry reduces the  
overestimation of SO<sub>2</sub> simulation, and the NMB decreases from 28.4% to 12.2%. The simulation of PM<sub>2.5</sub> changes from an  
underestimation to a slight overestimation, with the NMB changing from -34.6% to 3.8%. The R at the time of cloud chemistry  
simulation is also improved compared to the simulation without cloud chemistry. In conclusion, cloud chemistry can  
275 effectively reduce the model's overestimation of SO<sub>2</sub> and underestimation of PM<sub>2.5</sub>.

### 3.3 Site evaluation of cloud chemistry

Representative sites of Beijing, Nanjing, Guangzhou and Chengdu at NCP, YRD, PRD and SCB were selected to quantify  
the impact of cloud chemistry during the pollution episode. The net depletion ratio of SO<sub>2</sub> column concentration (RT(SO<sub>2</sub>))  
during cloud chemistry is shown in Figure 9. It is found that SO<sub>2</sub> column concentration reduction maintained mostly a high  
280 value of over 70%, even to 80% sometimes, in Chengdu from 17<sup>th</sup> to 21<sup>st</sup>. In Nanjing, the SO<sub>2</sub> level was reduced by about 10%  
during the time from 17<sup>th</sup> to 19<sup>th</sup> and up to 70% from 20<sup>th</sup> to 21<sup>st</sup> when the episode matures there. The changes of SO<sub>2</sub> in these



two cities are consistent with the changes in cloud and liquid cloud water content distributions during the pollution period in Figure 3. The SO<sub>2</sub> reduction in Beijing and Guangzhou is below 20% for most time and is consistently maintained at around 10%. The lower oxidative transformation is related to the lower liquid water content in Beijing, while in Guangzhou it is attributed to the combination of low pollution levels and low cloud water content. Figure 3 shows that Chengdu maintained abundant water vapor conditions from 17<sup>th</sup> to 21<sup>st</sup>, and so does Nanjing from 20<sup>th</sup> to 21<sup>st</sup>. However, the ambient water vapor content is quite low in Guangzhou and Beijing throughout the process, so the SO<sub>2</sub> oxidation is much lower than that of Chengdu and Nanjing. In conclusion, the cloud chemistry process can lead to SO<sub>2</sub> column concentration consumption share of more than 70% when cloud water content is abundant, which is also consistent with the observations of Mount Tai by Li (2020).

The effect of cloud chemistry on surface SO<sub>2</sub> and sulfate in four sites are also shown in Figure 10. The overall trend shows that the peak and valley regions of surface SO<sub>2</sub> consumption and sulfate increase are coincident. The cloud chemical processes make the surface SO<sub>2</sub> oxidation vary greatly between cities in different regions (Fig. 10a). The percentage of surface SO<sub>2</sub> consumption can reach more than 90% from 16<sup>th</sup> to 21<sup>st</sup> in Chengdu and Nanjing, while in Beijing and Guangzhou it is below 10%, reaching 20% until 22<sup>nd</sup>. Although the percentage of surface SO<sub>2</sub> consumption varies greatly, the increase in the percentage of sulfate in different cities does not vary that much. The increase in surface sulfate (Fig. 10b) was between 60% and 80% in Chengdu on the 19<sup>th</sup> to 21<sup>st</sup>, between 80% and 100% in Nanjing on the 20<sup>th</sup> to 21<sup>st</sup>, between 50% and 80% in Guangzhou, and between 20% and 40% in Beijing. The increase ratios of sulfate by cloud chemistry in Chengdu and Nanjing, where the influence of cloud chemistry is more evident than that in other two cities, are consistent with the results of Turnock et al. (2019).

Figure 11 is the variation of vertical profiles of sulfate increase at the four sites at 12:00 and 21:00 LST on 20 Dec., 17:00 LST on the 21 Dec. and 12:00 LST on the 22 Dec.. It shows that the sulfate produced by cloud chemistry during this pollution process is concentrated mostly below 5 km in the troposphere. Again, more sulfate has been produced in Chengdu and Nanjing in vertical than that of Beijing and Guangzhou, especially under 2 km in the troposphere.

#### 4. Summary and conclusions

The cloud chemistry mechanism in WRF/CUACE has been assessed by using the in-situ cloud chemistry observations of SO<sub>2</sub>, O<sub>3</sub>, and H<sub>2</sub>O<sub>2</sub> from Mount Tai in June-July 2015 and 2018. The results show that the mechanism well captures the cloud processes for the oxidation of SO<sub>2</sub>, reducing SO<sub>2</sub> by more than 80% during the cloudy phase of heavy pollution, which is in good agreement with the observations.



310 The assessment of cloud chemistry contributions to the changes of SO<sub>2</sub> and sulfate in NCP, YRD, PRD and SCB regions  
by WRF/CUACE revealed that except for PRD, all other three regions are significantly affected by the cloud chemistry, of  
which the SCB is the most obvious, with the strongest SO<sub>2</sub> abatement and sulfate increase, averaging up to 1-15 ppb for SO<sub>2</sub>  
abatement and more than 20 µg/m<sup>3</sup> with up to more than 50 µg/m<sup>3</sup> for sulfate increase in the central. Although the average  
effect of cloud chemistry is much weaker in the NCP with less water vapor in December, the contribution of the southern part  
315 of NCP during heavy pollution time is still significant and cannot be ignored. In PRD, the contribution of cloud chemistry is  
weaker than other regions due to lighter pollution, although there are many clouds with more water vapor there. In addition,  
surface sulfate increases by 40-80% in Beijing, Nanjing, Chengdu and Guangzhou in December during heavy pollution, similar  
to that of previous studies (Turnock et al., 2019). Above all, the average contribution of cloud chemistry during the pollution  
period was significantly greater than that for all December. Vertically, the analysis of the pollution process for the 2016 winter  
320 heavy pollution episode showed that the cloud chemistry influence was mainly in the middle and lower troposphere below 5  
km for 4 representative cities. Generally, the cloud chemistry improved the model performance by reducing the SO<sub>2</sub>  
overestimates and enhancing the correlations with observations for both SO<sub>2</sub> and sulfate.

This paper has been focused on the cloud chemical mechanism evaluation, and assessed the contribution of cloud  
chemistry to SO<sub>2</sub> and sulfate changes. In the future, more mechanisms should be added to improve the cloud chemistry  
325 mechanism in CUACE to more accurately simulate SO<sub>2</sub> and sulfate and other aerosol components such as nitrate, ammonium,  
carbonate, and organic aerosols.

#### **Code/data availability**

All source code and data can be accessed by contacting the corresponding authors Sunling Gong ([gongsl@cma.gov.cn](mailto:gongsl@cma.gov.cn)).

#### **Authors contribution**

330 CZ and SG put forward the ideas and formulated overarching research goals. JL carried them out and wrote the manuscript  
with suggestions from all authors. LZ and JZ participated in the scientific interpretation and discussion. JC assisted with data  
acquisition and processing. All authors contributed to the discussion and improvement of the manuscript.

#### **Competing interests**

The authors declare that they have no conflict of interest.

#### **Acknowledgements**

335 The authors would like to thank the Shanghai Key Laboratory of Atmospheric Particle Pollution and Prevention of Fudan



University for providing O<sub>3</sub>, SO<sub>2</sub> and H<sub>2</sub>O<sub>2</sub> datas at Mount Tai during cloudy periods.

#### **Financial support**

This research has been supported by the National Key Project of the Ministry of Science and Technology of  
340 China(2022YFC3700303); CMA Innovation Development Project (CXFZ2021J023).



## References

- Buchard, V., da Silva, A. M., Colarco, P., Krotkov, N., Dickerson, R. R., Stehr, J. W., Mount, G., Spinei, E., Arkinson, H. L., and He, H.: Evaluation of GEOS-5 sulfur dioxide simulations during the Frostburg, MD 2010 field campaign, *Atmospheric Chemistry and Physics*, 14, 1929-1941, <https://doi.org/10.5194/acp-14-1929-2014>, 2014.
- Caffrey, P., Hoppel, W., Frick, G., Pasternack, L., Fitzgerald, J., Hegg, D., Gao, S., Leaitch, R., Shantz, N., Albrechtski, T., and Ambrusko, J.: In-cloud oxidation of SO<sub>2</sub> by O<sub>3</sub> and H<sub>2</sub>O<sub>2</sub>: Cloud chamber measurements and modeling of particle growth, *Journal of Geophysical Research: Atmospheres*, 106, 27587-27601, <https://doi.org/10.1029/2000jd900844>, 2001.
- Charlson, R. J., Schwartz, S., and S., E.: Climate forcing by anthropogenic aerosols, *Science*, 255, 423-423, <https://doi.org/10.1126/science.255.5043.423>, 1992.
- Emery, C., Tai, E., and Yarwood, G.: Enhanced meteorological modeling and performance evaluation for two Texas ozone episodes, 2001.
- Ervens, B.: Modeling the Processing of Aerosol and Trace Gases in Clouds and Fogs, *Chemical Reviews*, 115, 4157-4198, <https://doi.org/10.1021/cr5005887>, 2015.
- Faloona, I., Conley, S. A., Blomquist, B., Clarke, A. D., Kapustin, V., Howell, S., Lenschow, D. H., and Bandy, A. R.: Sulfur dioxide in the tropical marine boundary layer: dry deposition and heterogeneous oxidation observed during the Pacific Atmospheric Sulfur Experiment, *Journal of Atmospheric Chemistry*, 63, 13-32, <https://doi.org/10.1007/s10874-010-9155-0>, 2010.
- Gao, M., Carmichael, G. R., Wang, Y., Ji, D., Liu, Z., and Wang, Z.: Improving simulations of sulfate aerosols during winter haze over Northern China: the impacts of heterogeneous oxidation by NO<sub>2</sub>, *Frontiers of Environmental Science & Engineering*, 10, 11, <https://doi.org/10.1007/s11783-016-0878-2>, 2016.
- Ge, W., Liu, J., Yi, K., Xu, J., Zhang, Y., Hu, X., Ma, J., Wang, X., Wan, Y., Hu, J., Zhang, Z., Wang, X., and Tao, S.: Influence of atmospheric in-cloud aqueous-phase chemistry on global simulation of SO<sub>2</sub> in CESM2, *Atmospheric Chemistry and Physics*, <https://doi.org/10.5194/acp-2021-406>, 2021.
- Georgiou, G. K., Christoudias, T., Proestos, Y., Kushta, J., Hadjinicolaou, P., and Lelieveld, J.: Air quality modelling in the summer over the eastern Mediterranean using WRF-Chem: chemistry and aerosol mechanism intercomparison, *Atmospheric Chemistry and Physics*, 18, 1555-1571, <https://doi.org/10.5194/acp-18-1555-2018>, 2018.
- Gong, S., and Zhang, X.: CUACE/Dust—an integrated system of observation and modeling systems for operational dust forecasting in Asia, *Atmospheric Chemistry and Physics*, 8, 2333-2340, <https://doi.org/10.5194/acp-8-2333-2008>, 2008.
- Gong, S. L., Barrie, L. A., Blanchet, J.-P., von Salzen, K., Lohmann, U., Lesins, G., Spacek, L., Zhang, L. M., Girard, E., Lin, H., Leaitch, R., Leighton, H., Chylek, P., and Huang, P.: Canadian Aerosol Module: A size-segregated simulation of atmospheric aerosol processes for climate and air quality models 1. Module development, *Journal of Geophysical Research*, 108, <https://doi.org/10.1029/2001jd002002>, 2003.
- Guo, J., Wang, Y., Shen, X., Wang, Z., Lee, T., Wang, X., Li, P., Sun, M., Jeffrey, L., Collett, J., Wang, W., and Wang, T.: Characterization of cloud water chemistry at Mount Tai, China: Seasonal variation, anthropogenic impact, and cloud processing, *Atmospheric Environment*, 60, 467-476, <https://doi.org/10.1016/j.atmosenv.2012.07.016>, 2012.
- Harris, E., Sinha, B., van Pinxteren, D., Tilgner, A., Fomba, K. W., Schneider, J., Roth, A., Gnauk, T., Fahlbusch, B., Mertes, S., Lee, T., Collett, J., Foley, S., Borrmann, S., Hoppe, P., and Herrmann, H.: Enhanced role of transition metal ion catalysis during in-cloud oxidation of SO<sub>2</sub>, *Science*, 340, 727-730, <https://doi.org/10.1126/science.1230911>, 2013.
- He, J., Zhang, Y., Glotfelty, T., He, R., Bennartz, R., Rausch, J., and Sartelet, K.: Decadal simulation and comprehensive evaluation of CESM/CAM5.1 with advanced chemistry, aerosol microphysics, and aerosol-cloud interactions, *Journal of Advances in Modeling Earth Systems*, 7, 110-141, <https://doi.org/10.1002/2014ms000360>, 2015.
- Hung, H. M., Hsu, M. N., and Hoffmann, M. R.: Quantification of SO<sub>2</sub> Oxidation on Interfacial Surfaces of Acidic Micro-Droplets: Implication for Ambient Sulfate Formation, *Environ Sci Technol*, 52, 9079-9086,



- 385 <https://doi.org/10.1021/acs.est.8b01391>, 2018.  
Kotarba, A. Z.: Calibration of global MODIS cloud amount using CALIOP cloud profiles, *Atmospheric Measurement Techniques*, 13, 4995-5012, <https://doi.org/10.5194/amt-13-4995-2020>, 2020.  
Lelieveld, Jos, Heintzenberg, and Jost: Sulfate cooling effect on climate through in-cloud oxidation of anthropogenic SO<sub>2</sub>, *Science*, <https://doi.org/10.1126/science.258.5079.117>, 1992.
- 390 Li, J. R.: Microphysical Characteristics and S(IV) Multiphase Chemical Reaction Mechanism of Orographic Clouds, Ph.D. thesis, Fudan University, 127pp, 2020.  
Li, J., Wang, X., Chen, J., Zhu, C., Li, W., Li, C., Liu, L., Xu, C., Wen, L., Xue, L., Wang, W., Ding, A., and Herrmann, H.: Chemical composition and droplet size distribution of cloud at the summit of Mount Tai, China, *Atmospheric Chemistry and Physics*, 17, 9885-9896, <https://doi.org/10.5194/acp-17-9885-2017>, 2017.
- 395 Li, J., Zhu, C., Chen, H., Fu, H., Xiao, H., Wang, X., Herrmann, H., and Chen, J.: A More Important Role for the Ozone - S(IV) Oxidation Pathway Due to Decreasing Acidity in Clouds, *Journal of Geophysical Research: Atmospheres*, 125, <https://doi.org/10.1029/2020jd033220>, 2020a.  
Li, J., Zhu, C., Chen, H., Zhao, D., Xue, L., Wang, X., Li, H., Liu, P., Liu, J., Zhang, C., Mu, Y., Zhang, W., Zhang, L., Herrmann, H., Li, K., Liu, M., and Chen, J.: The evolution of cloud and aerosol microphysics at the summit of Mt. Tai, China, *Atmospheric Chemistry and Physics*, 20, 13735-13751, <https://doi.org/10.5194/acp-20-13735-2020>, 2020b.
- 400 Li, M., Liu, H., Geng, G., Hong, C., Liu, F., Song, Y., Tong, D., Zheng, B., Cui, H., Man, H., Zhang, Q., and He, K.: Anthropogenic emission inventories in China: a review, *Natl. Sci. Rev.*, 4, 834-866, <https://doi.org/10.1093/nsr/nwx150>, 2017.  
Liu, S. C., McKeen, S. A., Hsie, E.-Y., Lin, X., Kelly, K. K., Bradshaw, J. D., Sandholm, S. T., Browell, E. V., Gregory, G. L., Sachse, G. W., Bandy, A. R., Thornton, D. C., Blake, D. R., Rowland, F. S., Newell, R., Heikes, B. G., Singh, H., and R. W. Talbot: Model study of tropospheric trace species distributions during PEM-WEST A, *J. Geophys. Res.*, 101, <https://doi.org/10.1029/1996JD002277>, 1996.
- 405 Li, P. F.: Fog Water Chemistry and Fog-Haze Transformation in Shanghai, Fudan University, Ph.D. thesis, 145pp.  
Liu, T., Chan, A. W. H., and Abbatt, J. P. D.: Multiphase Oxidation of Sulfur Dioxide in Aerosol Particles: Implications for Sulfate Formation in Polluted Environments, *Environ Sci Technol*, 55, 4227-4242, <https://doi.org/10.1021/acs.est.0c06496>,  
410 2021.  
Maahs, H. G.: Kinetics and Mechanism of the Oxidation of S(IV) by Ozone in Aqueous Solution With Particular Reference to SO<sub>2</sub> Conversion in Nonurban Tropospheric Clouds, *Journal of Geophysical Research*, 88, 10721-10732, <https://doi.org/10.1029/JC088iC15p10721>, 1983.  
Martin, G. M., D. W. Johnson, and A. Spice, The measurement and parameterization of effective radius in warm stratocumulus cloud, *J. Atmos. Sci.*, 51, 1823-1842, [https://doi.org/10.1175/1520-0469\(1994\)051<1823:TMAPOE>2.0.CO;2](https://doi.org/10.1175/1520-0469(1994)051<1823:TMAPOE>2.0.CO;2), 1994.
- 415 Molina: Air Quality in the Mexico Megacity: An Integrated Assessment, Alliance for Global Sustainability Bookseries, <https://doi.org/10.1007/978-94-010-0454-1>, 2002.  
Pye, H. O. T., Nenes, A., Alexander, B., Ault, A. P., Barth, M. C., Clegg, S. L., Jr., J. L. C., Fahey, K. M., Hennigan, C. J., Herrmann, H., Kanakidou, M., Kelly, J. T., Ku, I.-T., McNeill, V. F., Riemer, N., Schaefer, T., Shi, G., Tilgner, A., Walker, J. T.,  
420 Wang, T., Weber, R., Xing, J., Zaveri, R. A., and Zuend, A. A.: Havaia O. T. Pye The acidity of atmospheric particles and clouds, *Atmospheric Chemistry Physics*, 20, 4809-4888, <https://doi.org/10.5194/acp-20-4809-2020>, 2020.  
Ramanathan, V., Crutzen, P. J., Kiehl, J. T., and Rosenfeld, D.: Aerosols, climate, and the hydrological cycle, *Science*, 294, 2119-2124, [10.1126/science.1064034](https://doi.org/10.1126/science.1064034), 2001.  
Ravishankara, A. R.: Heterogeneous and Multiphase Chemistry in the Troposphere, *Science*, 276, 1058-1065, <https://doi.org/10.1126/science.276.5315.1058>, 1997.
- 425 Ren, Y., Ding, A., Wang, T., Shen, X., Guo, J., Zhang, J., Wang, Y., Xu, P., Wang, X., and Gao, J.: Measurement of gas-phase total peroxides at the summit of Mount Tai in China, *Atmospheric Environment*, 43, 1702-1711,



- <https://doi.org/10.1016/j.atmosenv.2008.12.020>, 2009.
- Sha, T., Ma, X., Jia, H., Tian, R., Chang, Y., Cao, F., and Zhang, Y.: Aerosol chemical component: Simulations with WRF-Chem and comparison with observations in Nanjing, *Atmospheric Environment*, 218, 430  
<https://doi.org/10.1016/j.atmosenv.2019.116982>, 2019.
- Shen, X., Lee, T., Guo, J., Wang, X., Li, P., Xu, P., Wang, Y., Ren, Y., Wang, W., Wang, T., Li, Y., Carn, S. A., and Collett, J. L.: Aqueous phase sulfate production in clouds in eastern China, *Atmospheric Environment*, 62, 502-511,  
<https://doi.org/10.1016/j.atmosenv.2012.07.079>, 2012.
- 435 Shimadera, H., Kondo, A., Shrestha, K. L., Kaga, A., and Inoue, Y.: Annual sulfur deposition through fog, wet and dry deposition in the Kinki Region of Japan - ScienceDirect, *Atmospheric Environment*, 45, 6299-6308,  
<https://doi.org/10.1016/j.atmosenv.2011.08.055>, 2011.
- Sielski, J., Kazirod-Wolski, K., Jozwiak, M. A., and Jozwiak, M.: The influence of air pollution by PM<sub>2.5</sub>, PM<sub>10</sub> and associated heavy metals on the parameters of out-of-hospital cardiac arrest, *Sci Total Environ*, 788, 147541,  
440 <https://doi.org/10.1016/j.scitotenv.2021.147541>, 2021.
- Tremblay, A., and Leighton, H.: A Three-Dimensional Cloud Chemistry Model, *Journal of Climate & Applied Meteorology*, 25, 652-671, [https://doi.org/10.1016/1352-2310\(96\)00063-5](https://doi.org/10.1016/1352-2310(96)00063-5), 1986.
- Turnock, S. T., Mann, G. W., Woodhouse, M. T., Dalvi, M., O'Connor, F. M., Carslaw, K. S., and Sprackle, D. V.: The Impact of Changes in Cloud Water pH on Aerosol Radiative Forcing, *Geophysical Research Letters*, 46, 4039-4048,  
445 <https://doi.org/10.1029/2019GL082067>, 2019.
- Twomey: Aerosols, clouds and radiation, *Atmospheric Environment*.part A.general Topics, 25, 2435-2442,  
[https://doi.org/10.1016/0960-1686\(91\)90159-5](https://doi.org/10.1016/0960-1686(91)90159-5), 1991.
- Twomey, S. A., Piepgrass, M., and Wolfe, T. L.: An assessment of the impact of pollution on the global cloud albedo, *Tellus B: Chemical and Physical Meteorology*, 36B, 356-366, <https://doi.org/10.1111/j.1600-0889.1984.tb00254.x>, 1984.
- 450 von Salzen, K., Leighton, H. G., Ariya, P. A., Barrie, L. A., Gong, S. L., Blanchet, J. P., Spacek, L., Lohmann, U., and Kleinman, L. I.: Sensitivity of sulphate aerosol size distributions and CCN concentrations over North America to SO<sub>x</sub> emissions and H<sub>2</sub>O<sub>2</sub> concentrations, *Journal of Geophysical Research: Atmospheres*, 105, 9741-9765,  
<https://doi.org/10.1029/2000jd900027>, 2000.
- Wang, H., Shi, G. Y., Zhang, X. Y., Gong, S. L., Tan, S. C., Chen, B., Che, H. Z., and Li, T.: Mesoscale modelling study of the interactions between aerosols and PBL meteorology during a haze episode in China Jing-Jin-Ji and its near surrounding region – Part 2: Aerosols' radiative feedback effects, *Atmospheric Chemistry and Physics*, 15, 6(2015-03-23), 14, 3277-3287,  
455 <https://doi.org/10.5194/acp-15-3257-2015>, 2015.
- Wei, Y., Chen, X., Chen, H., Li, J., Wang, Z., Yang, W., Ge, B., Du, H., Hao, J., Wang, W., Li, J., Sun, Y., and Huang, H.: IAP-AACM v1.0: a global to regional evaluation of the atmospheric chemistry model in CAS-ESM, *Atmospheric Chemistry and Physics*, 19, 8269-8296, <https://doi.org/10.5194/acp-19-8269-2019>, 2019.
- 460 Xie, Y., Dai, H., Zhang, Y., Wu, Y., Hanaoka, T., and Masui, T.: Comparison of health and economic impacts of PM<sub>2.5</sub> and ozone pollution in China, *Environ Int*, 130, 104881, <https://doi.org/10.1016/j.envint.2019.05.075>, 2019.
- Yao, S., Wang, Q., Zhang, J., and Zhang, R.: Characteristics of Aerosol and Effect of Aerosol-Radiation-Feedback in Handan, an Industrialized and Polluted City in China in Haze Episodes, *Atmosphere*, 12, 670, <https://doi.org/10.3390/atmos12060670>,  
465 2021.
- Ye, C., Xue, C., Zhang, C., Ma, Z., Liu, P., Zhang, Y., Liu, C., Zhao, X., Zhang, W., He, X., Song, Y., Liu, J., Wang, W., Sui, B., Cui, R., Yang, X., Mei, R., Chen, J., and Mu, Y.: Atmospheric Hydrogen Peroxide H<sub>2</sub>O<sub>2</sub> at the Foot and Summit of Mt Tai Variations Sources, *Journal of Geophysical Research: Atmospheres*, 126, <https://doi.org/10.1029/2020JD033975>, 2021.
- Yuan, D. M., Ma, X. H.: The severe haze process in 16–21 December 2016 and associated atmospheric circulation anomalies [J]. *Climatic and Environmental Research (in Chinese)*, 22 (6): 757–764, <https://doi.org/10.3878/j.issn.1006-9585.2017.17029>,  
470





- 2017.
- Zhang, L., Gong, S., Zhao, T. L., Zhou, C. H., and Zhang, X. Y.: Development of WRF/CUACE v1.0 model and its preliminary application in simulating air quality in China, *Geoscientific Model Development*, <https://doi.org/10.5194/gmd-14-703-2021>, 2021.
- 475 Zhang, X. Y., Wang, Y. Q., Niu, T., Zhang, X. C., Gong, S. L., Zhang, Y. M., and Sun, J. Y.: Atmospheric aerosol compositions in China: spatial/temporal variability, chemical signature, regional haze distribution and comparisons with global aerosols, *Atmospheric Chemistry and Physics*, 12, 779-799, <https://doi.org/10.5194/acp-12-779-2012>, 2012.
- Zheng, B., Tong, D., Li, M., Liu, F., Hong, C., Geng, G., Li, H., Li, X., Peng, L., Qi, J., Yan, L., Zhang, Y., Zhao, H., Zheng, Y., He, K., and Zhang, Q.: Trends in China's anthropogenic emissions since 2010 as the consequence of clean air actions, *Atmos.*
- 480 *Chem. Phys.*, 18, 14095-14111, <https://doi.org/10.5194/acp-18-14095-2018>, 2018.
- Zhou, C. H., Gong, S., Zhang, X. Y., Liu, H. L., Xue, M., Cao, G. L., An, X. Q., and Che, H. Z.: Towards the improvements of simulating the chemical and optical properties of Chinese aerosols using an online coupled model - CUACE/Aero, *Chemical and physical and meteorology*, <https://doi.org/10.3402/tellusb.v64i0.18965>, 2012.
- Zhou, C. H., Zhang, X. Y., Gong, S., Wang, Y. Q., and Xue, M.: Improving aerosol interaction with clouds and precipitation in a regional chemical weather modeling system, *Atmospheric Chemistry and Physics*, 16, 145-160, <https://doi.org/10.5194/acp-16-145-2016>, 2016.

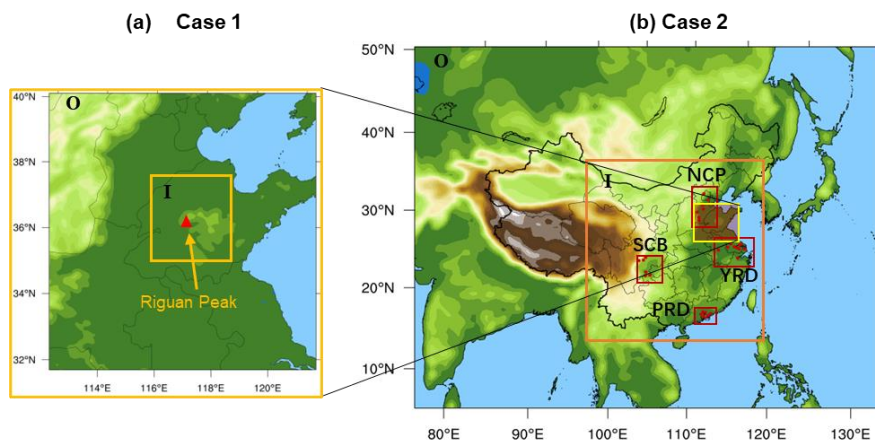


**Figure 1.** Model nesting domains and assessment regions: (a) finer grids for the Case 1, i.e., model evaluations. The red triangle is the Riguan Peak of the Mount Tai where the  $\text{SO}_2$ ,  $\text{O}_3$  and  $\text{H}_2\text{O}_2$  were observed, and (b) larger grids for regional assessment for Case 2. The sites with the surface observations of air pollutants are illustrated with red dots. Four regional assessment regions, i.e., NCP, YRD, PRD and SCB are also outlined.

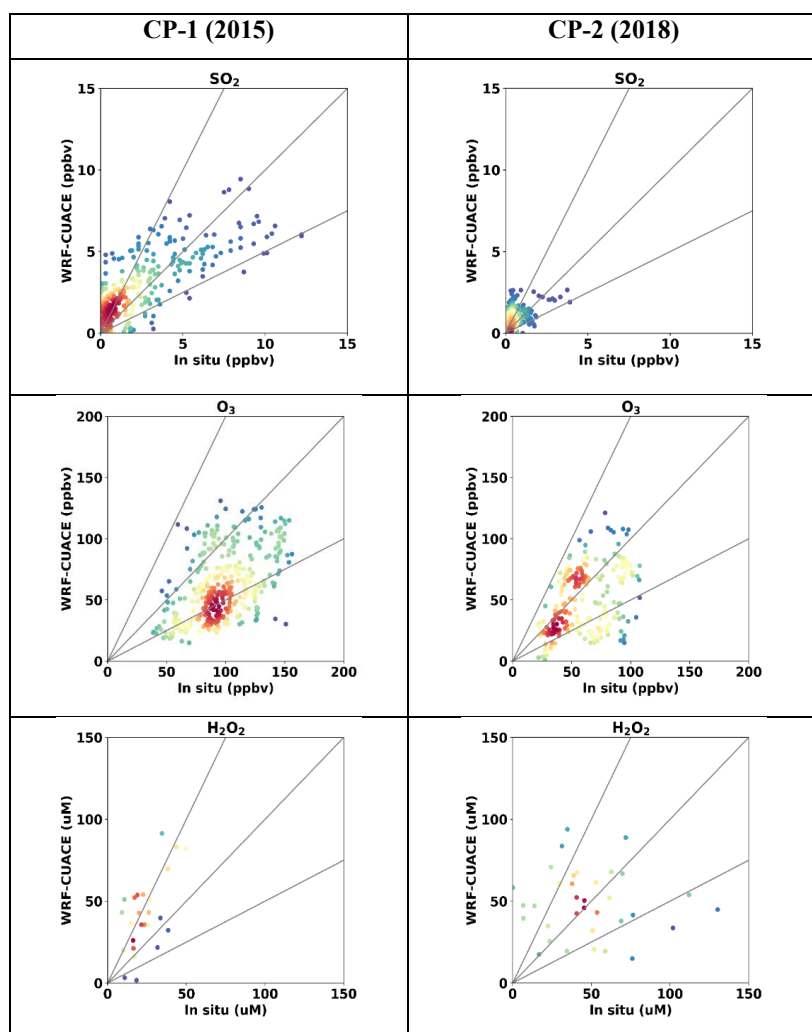
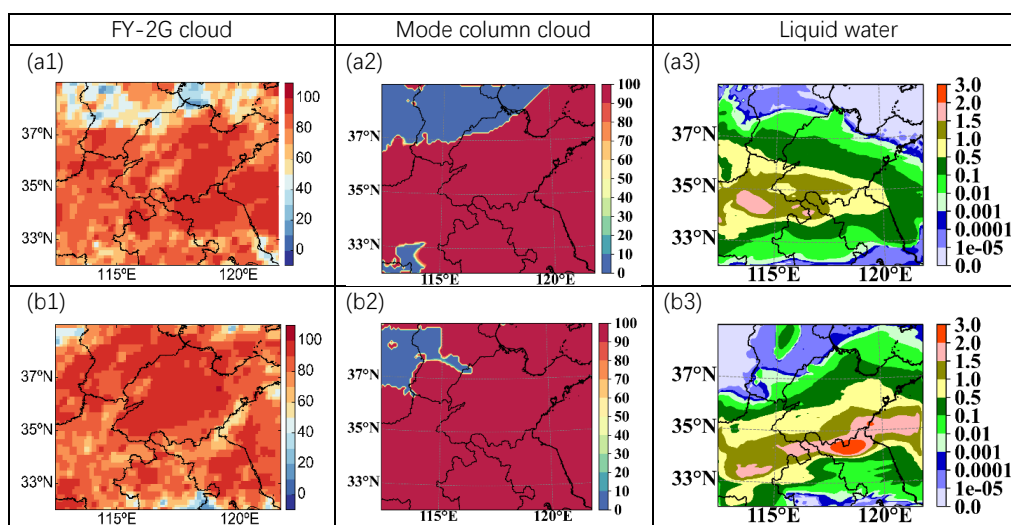


Figure 2. Scatter plots and correlation coefficients of hourly SO<sub>2</sub>, O<sub>3</sub> and H<sub>2</sub>O<sub>2</sub> concentrations between WRF/CUACE and in situ observations at Mount Tai.



**Figure 3.** (a1, b1): the cloud image of FY2G, (a2, b2): the cloud fraction by WRF/CUACE. (a3, b3): the liquid water content by WRF/CUACE (Units:  $\text{g m}^{-2}$ ). (a) is for 8:00 LST on 24 June, (b) is for 8:00 LST on 25 June.

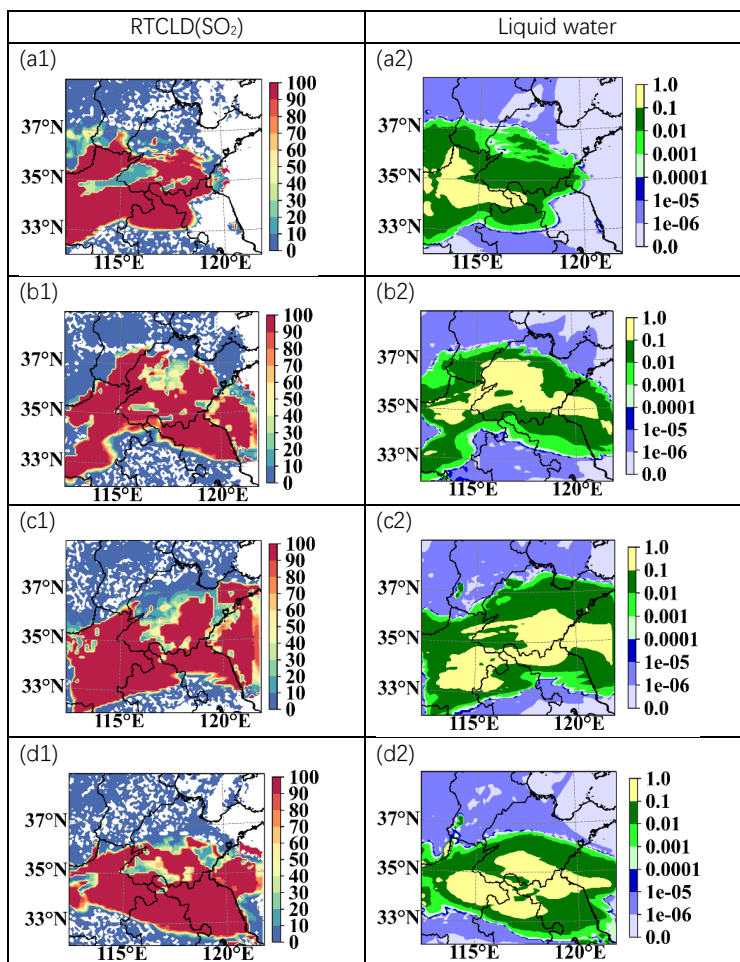
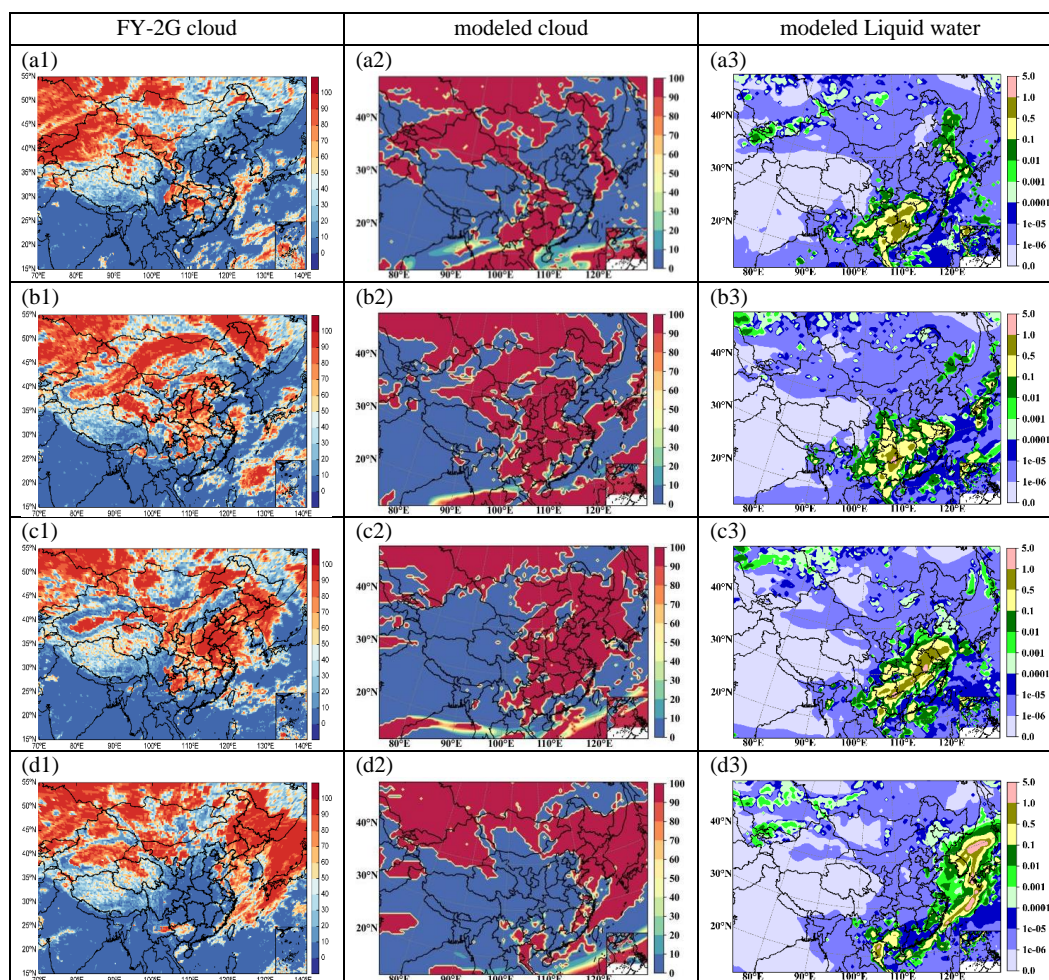
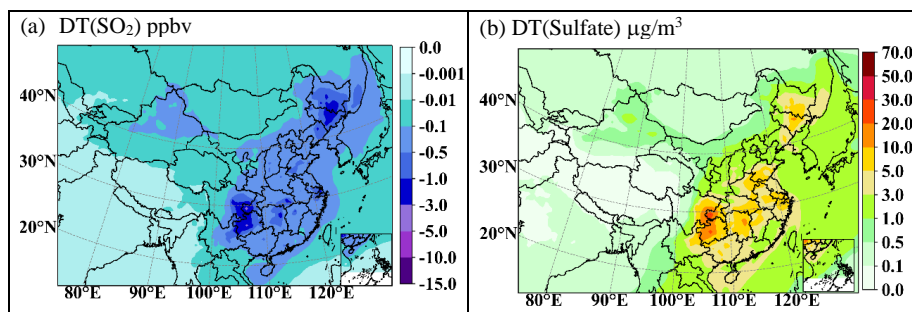


Figure 4. The percentage of SO<sub>2</sub> oxidized (a1, b1, c1 and d1) (%) and the liquid water content (a2, b2, c2 and d2) (g/kg) by WRF/CUACE, where (a) is for 2:00 LST on 24 June, (b) is for 8:00 LST on 24 June, (c) is for 2:00 LST on 25 June and (d) is for 8:00 LST on 25 June.



**Figure 5.** (a1, b1, c1, d1): the cloud image of FY-2G (%); (a2, b2, c2, d2): the column cloud of WRF/CUACE (%); (a3, b3, c3, d3): the liquid water content of WRF/CUACE ( $\text{g}/\text{m}^2$ ). (a) is for 8:00 LST on 19 Dec., (b) is for 8:00 LST on 20 Dec., (c) is for 8:00 LST on 21 Dec., and (d) is for 8:00 LST on 22 Dec.



**Figure 6.** The mean  $\text{SO}_2$  concentration decreased (a) and sulfate concentration increased (b) by cloud chemistry in Dec. 2016.



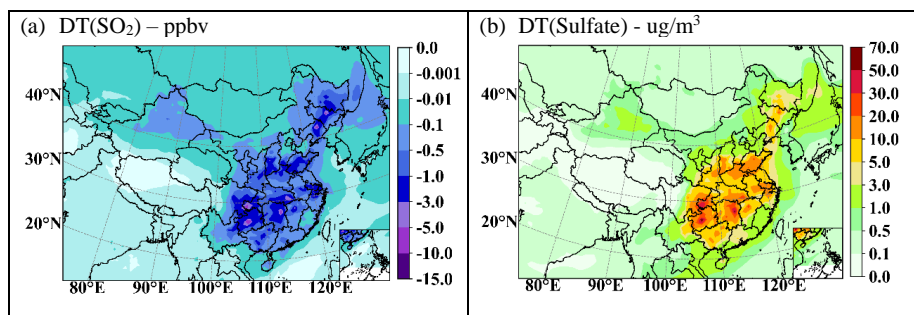


Figure 7. The mean  $\text{SO}_2$  concentration decreased (a) and sulfate concentration increased (b) by cloud chemistry from 19-21 Dec., 2016.

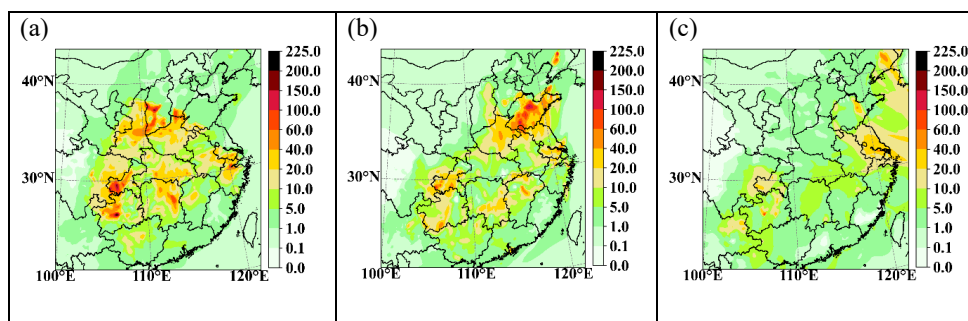


Figure 8. The differences in surface sulfate concentrations between with and without cloud chemistry at 21:00 on 20 Dec. (a), at 17:00 on 21 Dec. (b), and at 12:00 on 22 Dec. (c) ( $\mu\text{g}/\text{m}^3$ ).

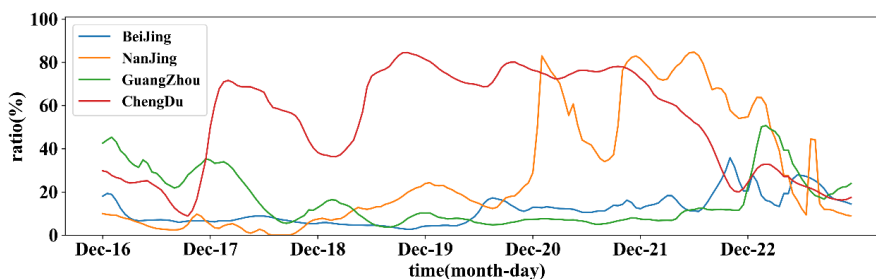


Figure 9. The percentage of  $\text{SO}_2$  column concentration reduced due to oxidation in cloud chemistry.

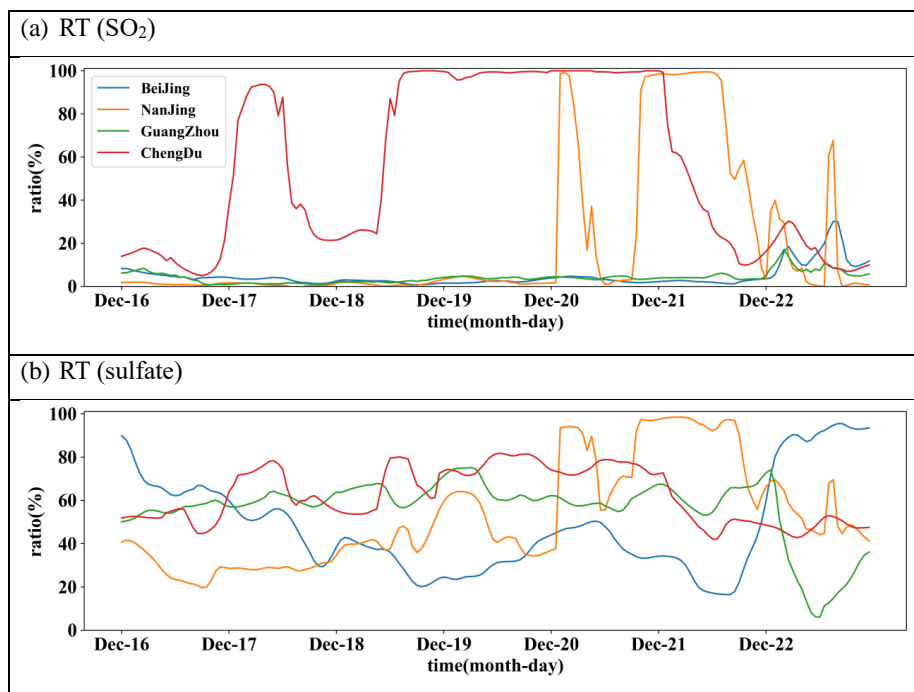


Figure 10. The percentage of surface SO<sub>2</sub> reduced (a) and the surface sulfate increased (b) influenced by cloud chemistry.

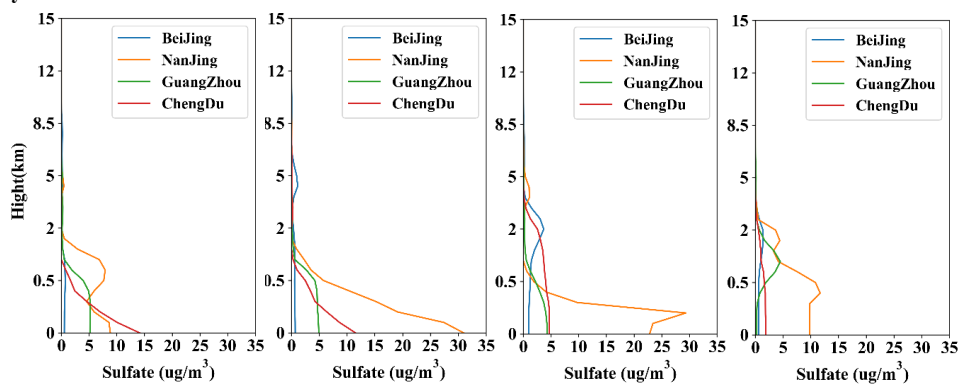


Figure 11. Vertical profile of sulfate concentration difference, i.e., DT (sulfate) at 12:00 on 20 Dec., at 21:00 on 20 Dec., at 17:00 on 21 Dec., and at 12:00 on 22 Dec.





**Table 1. Equilibrium Constants Used for the Parameterization of the Cloud Chemistry.**

Equilibrium Relation	Constant Expression	Equilibrium Constant		
		K(298)	a	Unit
$SO_2(g) + H_2O(aq) \leftrightarrow SO_2(aq)$	$K_{HS} = \frac{[SO_2(aq)]}{[SO_2(g)]}$	$1.23 \times 10^{-3}$	3120	$\frac{M}{atm}$
$SO_2(aq) \leftrightarrow H^+ + HSO_3^-$	$K_{1S} = \frac{[H^+][HSO_3^-]}{[SO_2(aq)]}$	$1.7 \times 10^{-2}$	2090	M
$HSO_3^- \leftrightarrow H^+ + SO_3^{2-}$	$K_{2S} = \frac{[H^+][SO_3^{2-}]}{[HSO_3^-]}$	$6.0 \times 10^{-8}$	1120	M
$O_3(g) + H_2O(aq) \leftrightarrow O_3(aq)$	$K_{HO} = \frac{[O_3(aq)]}{[O_3(g)]}$	$1.15 \times 10^{-2}$	2560	$\frac{M}{atm}$
$H_2O_2(g) + H_2O(aq) \leftrightarrow H_2O_2(aq)$	$K_{HP} = \frac{[H_2O_2(aq)]}{[H_2O_2(g)]}$	$9.7 \times 10^4$	6600	$\frac{M}{atm}$

**Table 2. physics parameterization schemes in WRF.**

Physical management	Parameterization	References
microphysics scheme	Lin	Lin et al. (1983)
shortwave radiation	Goddard	Chou and Suarez (1994)
longwave radiation	RRTM	Mlawer et al. (1997)
land surface scheme	Noah	Chen and Dudhia (2001)
boundary layer scheme	MYJ	Janjić (1994)
cumulus scheme	Grell-3D	Grell (1993)

**Table 3. Statistics for SO<sub>2</sub>, O<sub>3</sub> and H<sub>2</sub>O<sub>2</sub> in cloud chemistry at Mount Tai site.**

	Obs	Mod	R	RAD	NMB(%)
CP-1 SO <sub>2</sub> (ppbv)	2.16	2.54	0.77	-0.08	17.4%
CP-1 O <sub>3</sub> (ppbv)	97.79	61.70	0.49	0.23	-36.9%
CP-1 H <sub>2</sub> O <sub>2</sub> (uM)	26.52	49.11	0.72	-0.30	85.2%
CP-2 SO <sub>2</sub> (ppbv)	0.56	0.81	0.49	-0.18	44.9%
CP-2 O <sub>3</sub> (ppbv)	60.68	49.36	0.46	0.10	-18.7%
CP-2 H <sub>2</sub> O <sub>2</sub> (uM)	46.92	49.32	0.03	-0.02	5.1%



**Table 4. Statistical metrics for meteorology in NCP, YRD, PRD and SCB for Dec. 16-21 and the whole Dec. in 2016.**

		Obs		Mod		R		NMB(%)		RMSE	
		16-21	Dec.	16-21	Dec.	16-21	Dec.	16-21	Dec.	16-21	Dec.
NCP	T2(°C)	0.99	1.11	2.83	2.05	0.70	0.84	187.31%	84.94%	3.30	2.51
	RH2(%)	78.83	68.31	52.30	48.75	0.54	0.64	-33.66%	-28.63%	32.24	25.89
	WS10(m/s)	1.47	1.69	1.67	2.16	0.49	0.54	14.05%	27.46%	1.15	1.26
YRD	T2(°C)	9.24	7.99	9.51	8.40	0.94	0.96	2.85%	5.08%	1.42	1.29
	RH2(%)	79.22	75.62	73.81	72.98	0.86	0.85	-6.83%	-3.49%	10.70	9.26
	WS10(m/s)	2.16	2.27	2.78	2.99	0.74	0.76	28.74%	31.93%	1.23	1.30
PRD	T2(°C)	18.31	17.27	18.98	17.93	0.93	0.92	3.64%	3.80%	1.85	1.92
	RH2(%)	72.19	70.43	64.31	65.35	0.76	0.68	-10.91%	-7.21%	13.97	13.92
	WS10(m/s)	1.78	2.36	2.02	3.24	0.67	0.72	13.57%	37.14%	0.97	1.49
SCB	T2(°C)	10.18	9.70	10.46	9.99	0.74	0.75	2.77%	3.08%	1.82	2.15
	RH2(%)	81.63	79.92	74.09	71.26	0.66	0.60	-9.23%	-10.84%	12.71	15.52
	WS10(m/s)	1.09	1.27	1.63	1.92	0.49	0.36	49.18%	50.48%	1.03	1.28

**Table 5. Statistical metrics for hourly SO<sub>2</sub>, O<sub>3</sub> and PM<sub>2.5</sub> in NCP, YRD, PRD and SCB for Dec. 16-21 and the whole Dec. in 2016.**

		Obs		Mod		R		NMB(%)		RMSE	
		16-21	Dec.	16-21	Dec.	16-21	Dec.	16-21	Dec.	16-21	Dec.
NCP	SO <sub>2</sub> (ug/m <sup>3</sup> )	57.12	52.82	48.44	38.19	0.17	0.31	-15.2%	-27.7%	42.92	36.53
	O <sub>3</sub> (ug/m <sup>3</sup> )	11.15	15.46	9.35	11.16	0.35	0.55	-16.2%	-27.8%	13.05	14.60
	PM <sub>2.5</sub> (ug/m <sup>3</sup> )	319.30	186.66	296.41	196.24	0.40	0.59	-7.2%	5.1%	166.55	112.83
YRD	SO <sub>2</sub> (ug/m <sup>3</sup> )	22.37	19.55	22.48	19.82	0.55	0.42	0.5%	1.4%	13.09	12.81
	O <sub>3</sub> (ug/m <sup>3</sup> )	26.94	34.74	14.26	18.13	0.61	0.63	-47.1%	-47.8%	21.48	26.74
	PM <sub>2.5</sub> (ug/m <sup>3</sup> )	84.81	70.28	118.01	105.25	0.72	0.72	39.1%	49.8%	46.59	51.61
PRD	SO <sub>2</sub> (ug/m <sup>3</sup> )	15.19	15.18	28.45	19.51	0.46	0.35	87.3%	28.5%	21.36	13.30
	O <sub>3</sub> (ug/m <sup>3</sup> )	50.11	50.34	55.35	57.81	0.84	0.80	10.5%	14.8%	23.44	26.90
	PM <sub>2.5</sub> (ug/m <sup>3</sup> )	53.65	51.18	77.51	72.50	0.81	0.37	44.5%	41.7%	29.33	33.82
SCB	SO <sub>2</sub> (ug/m <sup>3</sup> )	22.03	20.31	16.55	12.49	0.32	0.24	-24.8%	-38.5%	14.58	14.72
	O <sub>3</sub> (ug/m <sup>3</sup> )	23.93	28.94	51.29	59.76	0.42	0.41	114.3%	106.5%	34.21	40.75
	PM <sub>2.5</sub> (ug/m <sup>3</sup> )	109.61	95.25	110.02	95.42	0.32	0.32	0.4%	0.2%	53.98	55.92

**Table 6. Statistical metrics for hourly SO<sub>2</sub> and PM<sub>2.5</sub> for sites in NCP, YRD, PRD and SCB defined in Figure 1 for Dec. 19-21.**

	Obs	Mod		R		NMB		RMSE	
		CLD	CCLD	CLD	CCLD	CLD	CCLD	CLD	CCLD
SO <sub>2</sub> (mg/m <sup>3</sup> )	29.3	32.8	37.6	0.41	0.34	12%	28%	30.5	34.3
PM <sub>2.5</sub> (mg/m <sup>3</sup> )	183.3	190.2	119.8	0.73	0.65	4%	-35%	121.1	150